archives
of thermodynamics
Vol. **44**(2023), No. 3, 83–98
DOI: 10.24425/ather.2023.147538

Thermodynamic analysis of hybrid ceramic bearings with metal inner rings

JIAN SUN[a]
GUANGXIANG ZHANG[a]
JUNXING TIAN[a*]
YUSHENG ZHU[b]

[a] School of Mechanical Engineering, Shenyang Jianzhu University, Liaoning, 100084, China

[b] Nanjing Metro Operation Co., Ltd., Nanjing 210000, China

Abstract For the sake of exploring the thermodynamic characteristics of hybrid ceramic bearings with metal inner rings in the application process, we established the mathematical model of bearings with metal inner rings based on the thermodynamics of bearings. The heat of the bearings, inner and outer raceway, and the deformation of bearings were calculated by the thermodynamic model. We used the bearing life testing machine to test the bearing load and speed. The consequences indicate that the temperature stability time of a hybrid ceramic bearing with the metal inner ring is about 6 hours after loading, and its temperature is about 1–2°C higher than that of a metal bearing. Under the condition of a certain speed, the stable temperature of bearing operation improves with the enlargement of the load. Under the condition of a certain load, the bearing temperature also improves with the enlargement of bearing speed. The overall temperature trend of the bearing outer ring is unanimous with the overall temperature value calculated by the model. The maximum error is between 2.2 and 2.4°C. The thermodynamic analysis of hybrid bearings with metal inner rings is conducive to a better study of the effect of bearing material characteristics on bearing performance.

Keywords: Hybrid ceramic bearing; Silicon nitride; Inner ring metal; Bearing temperature rise

*Corresponding Author. Email: tianjunxingge@163.com

Nomenclature

a – bearing raceways contact along the half-shaft
c_n – sliding coefficient of friction between the cage and the inner and outer rings
$d_i,\ d_e$ – bearing inner and outer ring groove diameter
D_m – rolling element diameter
D_{pw} – bearing pitch diameter
d_n – bearing outer ring inner diameter
d_w – bearing inner ring outer diameter
$E_{(\eta)}$ – second type elliptic integral of the raceway contact zone
F_n – friction of bearing cages
f_0 – coefficient related to the bearing type and lubrication
f_1 – coefficient related to the bearing type and load
$H_{bi},\ H_{be}$ – friction between the cage and the inner and outer ring generates heat
H_g – frictional heat generation between the bearing rolling elements and the cage pocket bore
$H_i,\ H_e$ – heat generation in the inner and outer rings of the bearing
$H_{si},\ H_{se}$ – heat generated in the contact zone between the inner and outer rings of the bearing
M – frictional moment of the bearing
M_0 – frictional moment related to the bearing designation, the speed of the bearing and the lubrication medium
M_1 – load-related frictional moment
$M_i,\ M_e$ – frictional torque between the inner and outer rings of the bearing
M_s – frictional moment generated by the spin motion of the bearing
$M_{si},\ M_{se}$ – friction torque concerning raceway dimensions
n – bearing speed
n_m – rotation speed of the bearing rolling elements
P_1 – equivalent dynamic load of the bearing
Q – normal contact load between bearing rolling elements and raceways
Q_g – contact load between rolling elements and cages
W_c – rolling element angular velocity
$W_i,\ W_e$ – bearing inner and outer ring angular velocity
z – number of rolling bodies

Greek symbols

μ – coefficient of friction between the bearing raceway and the rolling elements
μ_b – coefficient of friction between the rolling elements and the cage
ν – lubrication and dynamic viscosity

1 Introduction

As an important supporting component, the rolling bearing is an important part of the high-speed spindle element, and the high-speed spindle element is a critical part of the high-speed machine tool. Its performance has

an important impact on machining accuracy of high-speed machine tools. At present, engineering ceramic materials such as silicon carbide (SiC), zirconia (ZrO_2), and silicon nitride (Si_3N_4) have excellent properties such as corrosion resistance, abrasion resistance, high-temperature resistance, low-temperature resistance, high hardness, high strength, low density, low expansion coefficient and good self-lubrication [1,2]. Silicon nitride (Si_3N_4) stands out among engineering ceramic materials due to its higher hardness, better wear resistance, and lower weight. It is considered to be the best alternative for bearing steel. Silicon nitride full ceramic ball bearings have the characteristics of high hardness, high wear resistance, lightweight, and high thermal steady state [3,4]. Under the conditions of the same load and speed, the maximum contact area between the bearing rolling element and the inner and outer rings of steel bearings is larger than that between the bearing rolling elements and the inner and outer rings of hybrid bearings. So the contact stress is higher than that of steel bearings. And the density of silicon nitride material is smaller than that of bearing steels [5]. As the rotor system of the spindle unit is mainly metal, the assembly accuracy of full ceramic bearings is very high. Hybrid ceramic ball bearings with only ceramic balls as rolling elements cannot fully demonstrate their pressure resistance and self-lubricating characteristics. So this paper proposes a kind of hybrid ceramic ball bearing with the outer ring and ball as silicon nitride ceramic and the inner ring as metal. This type of bearing can reduce the mismatch between metal and ceramic materials and can fully utilize the performance of ceramics.

Friction between materials is a root cause of thermogenesis. The frictional thermogenesis between internal components of bearings under heavy load, high speed, and other working conditions is the main reason for the formation of a thermal field during bearing operation [6]. The formation of the thermal field directly affects the service performance and life of the bearing. Because the operation state of bearings is complex, the formation of the bearing thermal field is closely related to its operating state. The working temperature and its distribution are important aspects of bearing condition monitoring, which directly affects the service performance and life of the system.

At present, many experts and scholars have conducted an in-depth study on the performance of hybrid ceramic bearings. Ohta and Satake [7] experimentally studied the vibration characteristics of full ceramic bearings, mixed ceramic bearings, and full steel bearings respectively. They found that the factors affecting the vibration of full ceramic bearings, mixed

ceramic bearings, and steel bearings were almost identical, but the overall vibration level of mixed ceramic bearings was larger than that of full ceramic bearings and all-steel bearings. Wang *et al.* [8] built a comprehensive dynamic model of ball bearings with structural flexible deformation as the focus and deduced the ring flexibility caused by the assembly state change of the bearing housing system. They analyzed the interaction mechanism between the ring and other bearing components. Ma *et al.* [9] proposed the dynamic model of the bearing-rotor system and established the same motion differential equation as the bearing assembly. They obtained the real-time coupling and synchronization solutions for the bearing and rotor model. Fang *et al.* [10] improved the quasi-static model of ball bearings and proposed a general mathematical model of DR-ACBA in three different configurations. They compared and analyzed the influence of preload, velocity, and load on the variation of nonlinear stiffness of DR-ACBB under different configurations. Hao *et al.* [11] established a new thermal mesh model for the dynamic temperature of bearings, discussed the coupling effect between lubricant characteristics, heat generation, structural parameters, and temperature during bearing operation, and finally realized and discussed the effects of speed, load, oil temperature, and lubricant flow on the temperature rise. Zhang *et al.* [12] used the Hertz theory to establish the dynamic and thermal coupling model of ceramic bearing electric spindle, studied the influence of different temperatures, preload, and speed on bearing dynamic performance, and verified the accuracy of the dynamic and thermal coupling model through the electric spindle test platform. Tian *et al.* [13] established a bearing heating model based on silicon nitride material, measured the bearing temperature by a bearing life testing machine, verified the correctness of the model, and used the friction and wear testing machine to analyze the temperature change trend between rolling elements and raceways with different precision. Chen *et al.* [14] established a bearing lubrication and heat generation model under oil-air lubrication conditions based on the theory of high-speed rolling bearings and two-phase flow, and further studied the effects of oil supply, lubricating oil viscosity, load, and speed on bearing temperature rise.

Currently, there is relatively little research on hybrid bearings based on an inner ring of metal and an outer ring and balls of ceramic. To deeply study the thermodynamic characteristics of such bearings, it is planned to first establish a mathematical model based on the characteristics of metal and ceramic materials, predict the temperature rise of the bearing, and

then use the life testing machine to test the bearing, analyze the test results, finally establish a finite element simulation model suitable for ceramic bearings, and further analyze the test results in combination with the test.

2 Model building and test methods

For the sake of better understanding the thermodynamic characteristics of hybrid ceramic bearings during operation, a thermodynamic model of bearings was established based on the material characteristics of ceramic materials and metal inner rings. Bearing-related parameters are shown in Table 1.

Table 1: Material characteristics

Material parameter	Units	Si_3N_4	GCr15
Density	$g{\cdot}cm^{-3}$	3.2	7.85
Coefficient of thermal expansion	K^{-1}	$3.5 \cdot 10^{-6}$	$3 \cdot 10^{-5}$
Modulus of elasticity	GPa	310	207
Poisson's ratio	–	0.26	0.30
Thermal conductivity	$W{\cdot}m^{-1}K^{-1}$	35	45

Friction torque due to lubricant viscosity when the bearing is unloaded is equal to

$$M_0 = \begin{cases} 160 \cdot 10^{-7} f_0 D_{pw}^3 & \text{for} \quad \nu n < 2000\,, \\ 10^{-7} f_0 (\nu n)^{2/3} D_{pw}^3 & \text{for} \quad \nu n \geq 2000\,, \end{cases} \tag{1}$$

where f_0 is the coefficient related to the bearing type and lubrication, ν is the dynamic viscosity of the lubricant, and n is the bearing speed. The load-dependent friction torque is

$$M_1 = f_1 P_1 D_{pw}\,, \tag{2}$$

where f_1 is the coefficient related to the bearing type and load, and P_1 refers to the bearing equivalent dynamic load. Therefore, the formula for the bearing friction torque is

$$M = M_0 + M_1\,. \tag{3}$$

During the operation process of angular contact ball bearings, the contact status between the rolling bodies and the inner and outer rings under the

action of centrifugal force is slightly different due to the high-speed rotation, resulting in different friction torque between the inner and outer rings [15]. Thus, according to the difference between bearing inner raceway diameter d_i and outer raceway diameter d_e, the total friction torque is divided. The friction torque of the inner ring is

$$M_i = 0.5\frac{MD_m}{d_i} \tag{4}$$

and the friction torque of the outer ring is

$$M_e = 0.5\frac{MD_m}{d_e}\,. \tag{5}$$

Because ceramic ball bearings are mostly used in high-speed rotation conditions, the spin sliding between the rolling body and the inner raceway of the bearing is one of the main movements during the working process of the bearing in addition to the inner ring rotation of the bearing and the rolling body rotation movement. The friction torque generated by spin sliding has a great effect on the total friction torque and should be considered when calculating thermogenesis. Therefore, the thermogenesis by spin sliding friction is added based on the above formula to make the empirical formula more accurate:

$$M_s = \frac{3\mu QaE_{(\eta)}}{8}\,, \tag{6}$$

where μ is the friction coefficient between the bearing raceway and the rolling body, and Q is the normal contact load between the bearing rolling body and the bearing raceway. The thermogenesis by the inner and outer rings and the contact area of the rolling body is related to the friction moment of the contact area and the rotation speed of the inner and outer rings and the rolling body. According to the diameter of the raceway, the spin friction moments M_s are divided into M_{se} and M_{si} related to the size of the raceway.

The thermogenesis by the inner ring is

$$H_i = 10^{-3}W_cM_i + 1.047\cdot 10^{-4}M_{si}n_mz \tag{7}$$

and the thermogenesis by the outer ring is

$$H_e = 10^{-3}W_cM_e + 1.047\cdot 10^{-4}M_{se}n_mz, \tag{8}$$

where z is the number of rolling bodies and W_c is the rolling element angular velocity.

Because the rolling body rotates around the centre of the bearing in the cage pocket, the angular speed of the cage is equal to the public angular speed of the rolling body. The friction thermogenesis between the rolling body and the cage pocket hole is

$$H_g = \mu_b Q_g W_c \,, \tag{9}$$

where μ_b is the friction coefficient between the rolling body and the cage, and Q_g is the contact load between the rolling body and the cage. Under high-speed rotation, the contact load Q_g between the rolling body and the cage is very small. So the friction thermogenesis between the rolling body and the cage can be ignored.

The movement of the cage is mainly guided by the friction between the cage and the rolling body or the inner and outer rings. When there is sliding friction between the cage and the outer ring, that is when the outer ring is guided, the thermogenesis by sliding friction between the cage and the outer ring is

$$H_{be} = 0.5 d_n F_n \left[c_n \left(W_c - W_e \right) \right], \tag{10}$$

where d_n is the inner diameter of the bearing outer ring, F_n is the friction force, c_n is the sliding friction coefficient and W_e is the outer angular velocity. When there is sliding friction between the cage and the inner ring, that is when the inner ring is guided, the thermogenesis by sliding friction between the cage and the inner ring is

$$H_{bi} = 0.5 d_n F_n \left[c_n \left(W_c - W_i \right) \right], \tag{11}$$

where d_w is the outer diameter of the inner ring and W_i is the inner angular velocity.

The total thermogenesis in the contact area of the inner and outer rings of the bearing is, respectively

$$\begin{aligned} H_{si} &= H_i + H_{bi} \,, \\ H_{se} &= H_e + H_{be} \,. \end{aligned} \tag{12}$$

3 Test methods

For the sake of studying the temperature variation characteristics of hybrid ceramic bearings during operation, we used the life testing machine for experimental research, as shown in Fig. 1. First of all, the test bearing

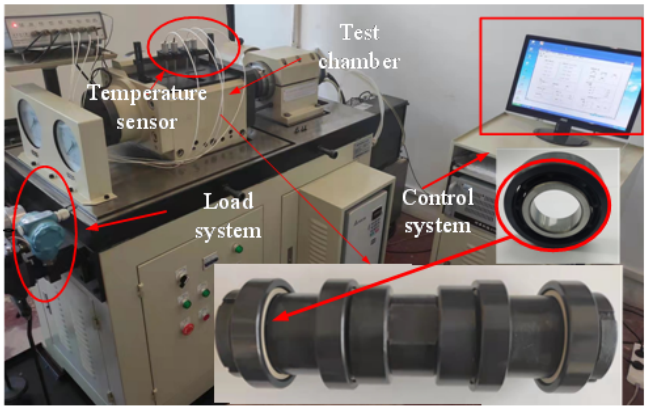

Figure 1: Life testing machine device diagram.

was soaked in the oil pollution cleaning agent to clean, to prevent pollutants from the bearing assembly process, affecting the operation state of the bearing. Then the test bearing was installed on the mandrel, and the mandrel was placed in the cavity of the bearing life testing machine. After the test bearing placement was completed, the bearing performance test was executed for the test parameters gathered in Table 2.

Table 2: Experimental parameters.

Working condition	Units	Value
Rotational speed	rpm	6000, 8000, 10000
Load	N	0, 500, 1000, 1500, 3000, 3500, 4000
Ambient temperature	°C	25
Lubrication	–	oil bath lubrication

As these hybrid ceramic bearings have the same inner ring as metal bearings, the outer ring, and balls are made of different materials, the thermal deformation of the shaft and the inner ring of the bearings are larger compared to the outer ring and balls when these bearings are used in conjunction with metal shafts. And the volume of change between the ball and the outer ring is relatively small. The thermal deformation of the shaft and bearing inner ring can be compensated by bearing clearance. However, the change of bearing clearance has a certain effect on the temperature rise of the bearing [16–20]. For the sake of studying the form of temperature change of hybrid ceramic bearing, the temperature rise of hybrid ceramic

bearing and metal bearing was compared, as shown in Fig. 2. Under the same operation condition, the initial temperature of the bearing is the same, but with the increase of operation time, the temperature of the bearing also rises. The temperature rise of metal bearings is lower than that of ceramic bearings. This is due to the relatively large thermal variables of the bearing inner ring and the shaft, while the thermal deformation of the ceramic ball and the ceramic outer ring is relatively small. Then the bearing heat dissipation space becomes smaller, and eventually, the temperature rises. In the process of operation of the bearing, its operation time is 6 hours, and the temperature of the bearing tends to be stable.

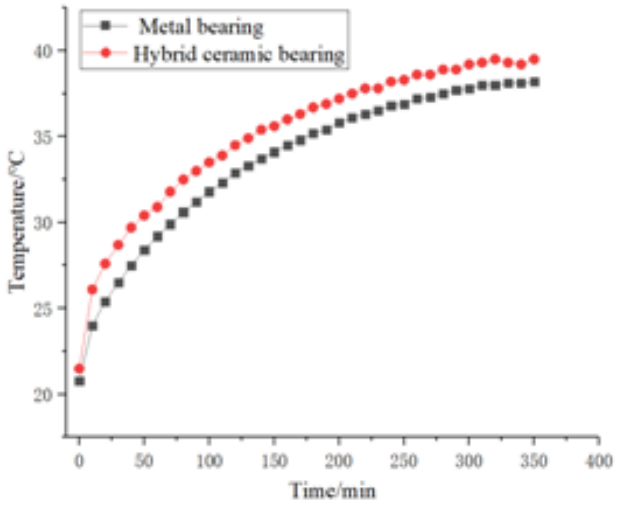

Figure 2: Test temperature of metal bearing and mixed ceramic bearing.

For the sake of studying the influence of load on the temperature of hybrid bearings, the speed of the life testing machine was set at 6000 rpm, and then the load as in Table 2 was applied. For the sake of obtaining the stable temperature of the bearings under each operation condition, each group of tests was operated for 8 h. The test consequences are indicated in Fig. 3. The consequences indicate that under the condition of a certain rotational speed, during stable operation of the bearing, its temperature increases with the increasing load. However, the heating process of the bearing is not obvious due to the influence of loading time and frequency. At bearing loads of 1500–4000 N, the stabilized temperature of the bearing during operation does not change much as the operating time increases. However, the

warming process of the bearing during operation is quite different. Under the condition that the bearing load is 4000 N, the operation temperature of the bearing rises relatively fast, and the highest temperature reaches 40°C. When the bearing is in no-load operation, the stable temperature of the bearing is about 37°C.

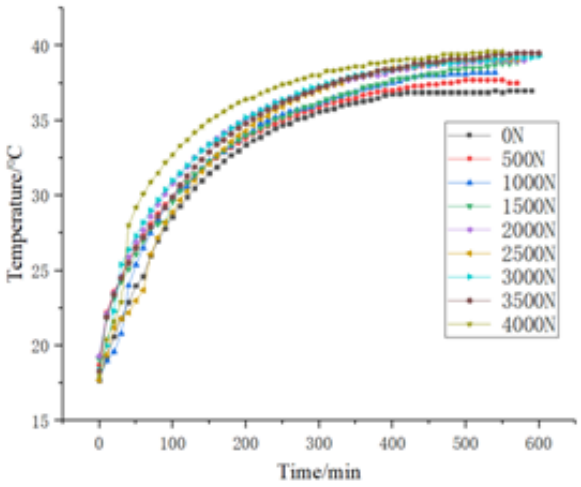

Figure 3: Influence of bearing load on temperature change.

To study the effect of the speed on the temperature of the hybrid bearing, the load of the life testing machine was assumed 1000 N, and the rotational speed was applied as in Table 2. The test consequences are indicated in Fig. 4. The consequences indicate that under a certain load, the temperature of the bearing increases with the rise of the bearing rotational speed. When the bearing speed is 10000 rpm, the highest temperature of the bearing reaches 45°C. When the bearing speed is 6000 rpm and 8000 rpm, the temperature changes are relatively smooth. This is because the friction frequency between the bearing ball and the inner and outer rings increases during the high-speed operation of the bearing, which makes the bearing temperature rise faster. However, after the bearing temperature reaches a stable value, it tends to be stable, and the temperature no longer rises, reaching a state of thermal equilibrium. The higher the rotational speed, the faster it takes to reach thermal equilibrium.

Since it is difficult to realize the test of bearing operation under high speed and heavy load conditions, the temperature change of bearing was

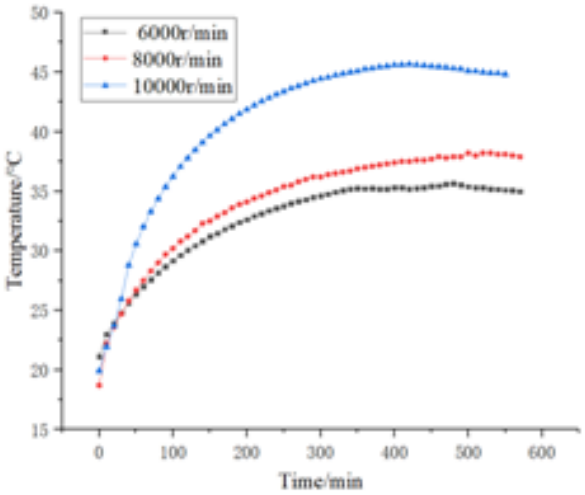

Figure 4: Influence of bearing speed on bearing temperature.

modelled, analyzed, and calculated. For the sake of verifying the accuracy of the model, we selected the rotational speed of 8000 rpm, and the load parameter as 0 N, 500 N, 1000 N, 1500 N, 2000 N, and 2500 N, and compared the obtained results with the experimental data. As can be seen from Fig. 5, the overall temperature trend of the bearing outer ring is consistent with the overall temperature value calculated by the model. The calculated

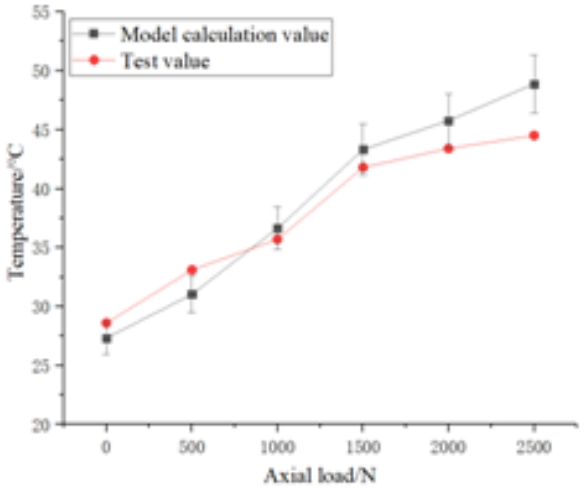

Figure 5: Analysis of test consequences and model consequences.

temperature of the bearing model and the test temperature are similar under the conditions of load 0 N, 500 N, 1000 N, and 1500 N. The error value is between 1.3 and 2°C, while the error for 2000 N and 2500 N is between 2.2 and 2.4°C. The error increases as the load increases, which is because the model has some error in calculating the amount of heat transfer in the calculation process.

The ball of the bearing, the inner raceway of the bearing, and the outer raceway of the bearing are difficult to measure during operation. The heat released in the bearing is generated under the action of torque between the ball and the inner and outer rings. To better understand the change of the temperature of the inner and outer ring of the hybrid bearing, based on the simulation model, the simulation analysis of the temperature change of the bearing under the condition of speed 8000 rpm and load 0–2500 N is made. The bearing simulation setup is shown in Fig. 6. The simulation procedure consists of the following steps:

1) set the material properties of each part and define the bearing assembly;
2) set the analysis step, power-display analysis, and turn on geometric nonlinearity;
3) divide the grid, using the C3D8R grid type;
4) set interaction, the ball is in face-to-face contact with the inner and outer ring and cage setting, the inner ring and the inner surface of the cage are coupled to the bearing centre, and the reference points RP1 and RP2 are set respectively;

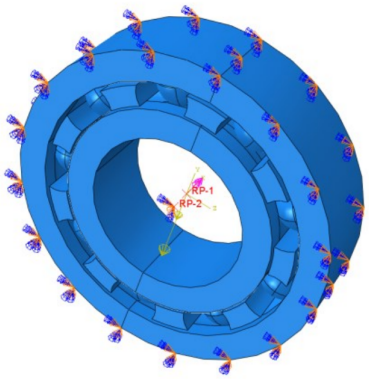

Figure 6: The bearing simulation setup.

5) apply load and boundary conditions, apply gravity as a whole, and apply force to the inner ring reference point RP1. The outer ring is fully fixed and angular velocity is applied to RP1 and RP2;

6) submit the job and run the analysis.

The simulation results are shown in Fig. 7. The temperature of the bearing ball and the inner and outer raceway increases with the increase of load. Using ABAQUS finite element analysis software, it was found that the highest temperature occurred in the position where the sphere is in contact with the channel – 65.61°C, as shown in Fig. 8. The high-temperature region of the inner and outer rings of the bearing is mainly concentrated in the raceway area. The temperature of the inner raceway is the same as that of the ball, but with the increase in load, the temperature difference between the ball and the inner raceway becomes larger, which is because of collection of heat from the inner raceway and the outer raceway. The heat generated by the ball is higher under the condition of large load. The temperature of the inner raceway of the bearing is higher than that of the outer raceway, and the maximum difference is 5°C. The overall simulation analysis of the bearing is shown in the figure, and the highest temperature point in the figure is at the position of the ball.

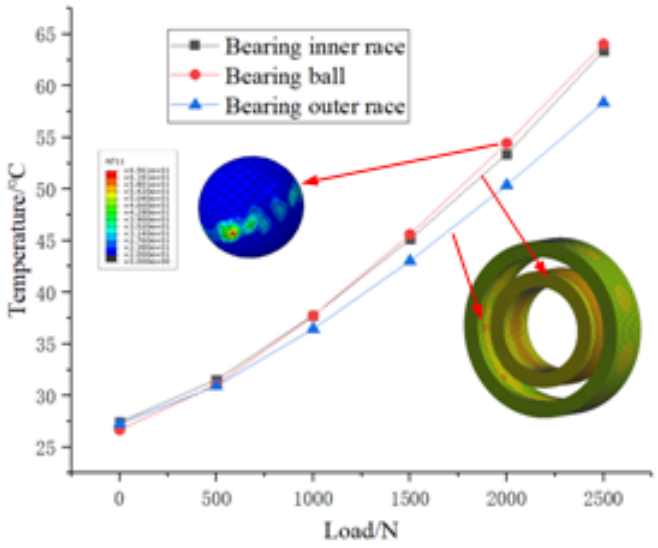

Figure 7: Analysis of temperature of bearing inner and outer rings and spheres.

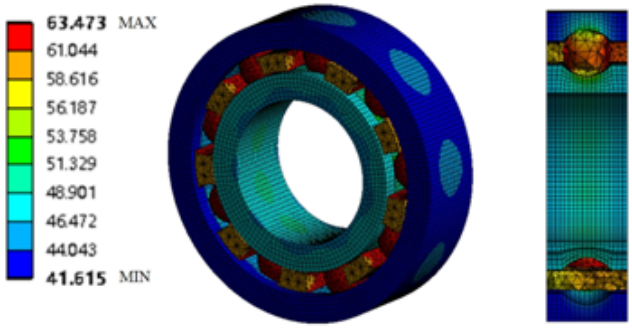

Figure 8: A Simulation analysis of the overall bearing temperature change.

4 Conclusion

The thermogenesis model of a hybrid bearing with the metal inner ring was established based on bearing thermodynamics, and the heat change of the bearing rolling body and the inner ring was analyzed. For the sake of studying the influence of bearing load and speed change on bearing thermogenesis, a bearing life testing machine was used to analyze and confirm the correctness of the simulation model.

1. Due to the relatively large thermal deformation of the inner ring and shaft of the bearing, the ceramic ball and ceramic outer ring have a relatively small thermal deformation. The clearance of the hybrid bearing becomes smaller, and then the heat dissipation space of the bearing becomes smaller, and finally, the temperature rises. Therefore, the temperature rise of hybrid bearings is relatively higher than that of metal bearings. After operation for 6 hours, the temperature of a hybrid ceramic bearing with a metal inner ring tends to be stable.
2. The stable operating temperature of the bearing increases with the rise of load. Under the condition of bearing load 4000 N, the operation temperature of the bearing rises relatively fast, and the highest temperature of the bearing reaches 40°C. When the bearing is in no-load operation, the stable temperature of the bearing is about 37°C.
3. Under the condition of a certain load, the temperature of the bearing rises with the rise of the bearing speed. When the bearing speed is 10000 rpm, the highest temperature of the bearing reaches 45°C. When the rotating speed is 6000 rpm and 8000 rpm, the temperature change is relatively smooth.

4. The temperature of the bearing ball is mainly focused on the contact position between the ball and the raceway, and the highest temperature is 65.61°C. The highest temperature of the inner and outer rings of the bearing is mainly on the raceway, and the temperature of the inner and outer raceway is the same as the temperature of the ball. However, with the rise of the load, the difference between the temperature of the ball and the inner raceway becomes larger. The temperature of the inner raceway of the bearing is higher than that of the outer raceway, and the maximum difference is 5°C.

Acknowledgments

The authors acknowledge the collective support granted by the National Natural Science Foundation of China (Grant No. 52105196), the Education Department of Liaoning Province (Grant No. LJKMZ20220936), Young and Middle-aged Innovation Team of Shenyang (Grant No. RC210343).

Received 15 March 2023

References

[1] Li S., Wei C., Wang Y.: *Fabrication and service of all-ceramic ball bearings for extreme conditions applications*. IOP Conf. Ser. Mat. Sci. Eng. **100**9(2021), 1, 012032. doi: 10.1088/1757-899X/1009/1/012032

[2] Xia Z., Wu Y., Wei H., Ren K., Gao L., Sun J., Li S.: *Experimental research on the influence of working conditions on vibration and temperature rise of Si3N4 full-ceramic bearing motors*. Shock Vib. **2021**(2021), 1–16. doi: 10.1155/2021/1176566

[3] Guo J., Wu Y., Zhang X., Zhang Y., Wang H., Bai X., Lu, H.: *Research on the influence of thermal expansion of steel shaft on dynamic characteristics of full ceramic bearing-rotor system*. Adv. Mech. Eng. **14**(2022), 7, 1–14. doi: 10.1177/16878132221109349

[4] Yan H., Wu Y., Li S., Zhang L., Zhang, K.: *The effect of factors on the radiation noise of high-speed full ceramic angular contact ball bearings*. Shock Vib. **2018**(2018), 1–9. doi: 10.1155/2018/1645878

[5] Han X., Xu C., Jin H., Xie W., Meng S.: *An experimental study of ultra-high temperature ceramics under tension subject to an environment with elevated temperature, mechanical stress and oxygen*. Sci. China Technol. Sc. **62**(2019), 1349–1356. doi: 10.1007/s11431-018-9501-1

[6] Wang Y., Cao J., Tong Q., An G., Liu R., Zhang Y., Yan H.: *Study on the thermal performance and temperature distribution of ball bearings in the traction motor of a high-speed EMU*. Appl. Sci. **10**(2020), 12, 4373. doi: 10.3390/app10124373

[7] Wang Y.Z., Liu H.B., Meng Y.G.: *Thermal field characteristics of lubrication under high-speed cylindrical roller bearing rings*. Aerosp. Power 36(2022), 5 (in Chinese). doi: 10.13224/j.cnki.jasp.20210583

[8] Wang M., Yan K., Tang Q., Guo J., Zhu Y., Hong J.: *Dynamic modeling and properties analysis for ball bearing driven by structure flexible deformations*. Tribol. Int. **179**(2023), 108163. doi: 10.1016/j.triboint.2022.108163

[9] Ma S., Yin Y., Chao B., Yan K., Fang B., Hong J.: *A Real-time Coupling Model of Bearing-Rotor System Based on Semi-flexible Body Element*. Int. J. Mech. Sci. **245**(2023), 108098. doi: 10.1016/j.ijmecsci.2022.108098

[10] Fang B., Zhang J., Hong J., Yan K.: *Research on the nonlinear stiffness characteristics of double-row angular contact ball bearings under different working conditions*. Lubricants. **11**(2023), 2, 44. doi: 10.3390/lubricants11020044

[11] Hao X., Yun X., Han Q.: *Thermal-fluid-solid coupling in thermal characteristics analysis of rolling bearing system under oil lubrication*. Tribol. **142**(2020), 3, 031201. doi: 10.1115/1.4045377

[12] Zhang K., Wang Z., Bai X., Shi H., Wang Q.: *Effect of preload on the dynamic characteristics of ceramic bearings based on a dynamic thermal coupling model*. Adv. Mech. Eng. **12**(2020), 1, 1687814020903851. doi: 10.1177/1687814020903851

[13] Tian J., Wu Y., Sun J., Xia Z., Ren K., Wang H., Yao J.: *Thermal dynamic exploration of full-ceramic ball bearings under the self-lubrication condition*. Lubricants **10**(2022), 9, 213. doi: 10.3390/lubricants10090213

[14] Chen C.Y., Li J.S., Yu Y.J., Xue Y.J.: *Study on temperature rise characteristics of oil-air lubrication of high-speed angular contact ball bearings*. Mach. Des. Manu. (2021), 9, 216–221+227 (in Chinese). doi: 10.19356/j.cnki.1001-3997.2021.09.049

[15] Wu Y., Ren K., Xia Z., Sun J., Tian J., Li S.: *Heat generation analysis of full-ceramic angular contact ball bearings under the condition of non-lubrication*. Mod. Mach. Tool Autom. Manufact. Techniq. (2022), 7, 148–151 (in Chinese). doi: 10.13462/j.cnki.mmtamt.2022.07.035

[16] Xia Z., Wu Y., Ma T., Bao Z., Tian J., Gao L., Li S.: *Experimental study on adaptability of full ceramic ball bearings under extreme conditions of cryogenics and heavy loads*. Tribol. Int. **175**(2022), 107849. doi: 10.1016/j.triboint.2022.107849

[17] Wang J., Xu M., Zhang C., Huang B., Gu F.: *Online bearing clearance monitoring based on an accurate vibration analysis*. Energies **13**(2020), 2, 389. doi: 10.3390/en13020389

[18] Shi H., Li Y., Bai X., Wang Z., Zou D., Bao Z., Wang Z.: *Investigation of the orbit-spinning behaviors of the outer ring in a full ceramic ball bearing-steel pedestal system in wide temperature ranges*. Mech. Syst. Signal Process. **149**(2021), 107317. doi: 10.1016/j.ymssp.2020.107317

[19] Smolík L., Hajžman M., Byrtus M.: *Investigation of bearing clearance effects in dynamics of turbochargers*. Int. J. Mech. Sci. **127**(2017), 62–72. doi: 10.1016/j.ijmecsci.2016.07.013

[20] Gu Y.K., Li W.F., Zhang J., Qiu G.Q.: *Effects of wear, backlash, and bearing clearance on dynamic characteristics of a spur gear system*. IEEE Access **7**(2019), 117639–117651. doi: 10.1109/ACCESS.2019.2936496